

Perfect Sampling of the Chemical Master Equation for Gene Regulatory Networks

Martin Hemberg and Mauricio Barahona*

Department of Bioengineering,
Imperial College London,
United Kingdom

Abstract

We present a Perfect Sampling algorithm that can be applied to the Master Equation of Gene Regulatory Networks (GRNs). The method recasts Gillespie's Stochastic Simulation Algorithm (SSA) in the light of Markov Chain Monte Carlo methods and combines it with the Dominated Coupling From The Past (DCFTP) algorithm to provide guaranteed sampling from the stationary distribution. We show how the DCFTP-SSA can be generically applied to genetic networks with feedback formed by the interconnection of linear enzymatic and nonlinear Monod- and Hill-type elements. We establish rigorous bounds on the error and convergence of the DCFTP-SSA, as compared to the standard SSA, through a set of increasingly complex examples. Once the building blocks for GRNs have been introduced, the algorithm is applied to study properly averaged dynamic properties of two experimentally relevant genetic networks: the toggle switch, a two-dimensional bistable system, and the repressilator, a six-dimensional genetic oscillator.

Key words: Perfect Sampling; Gillespie algorithm; Gene regulation.

*Corresponding author. Address: Department of Bioengineering, Imperial College London, South Kensington Campus, London, SW7 2AZ (United Kingdom); Telephone: +44 207 594 5189; Fax: +44 207 594 6897; e-mail: m.barahona@imperial.ac.uk

Introduction

The recent interest in stochastic models of chemical reactions has been largely motivated by experiments which have demonstrated the stochastic nature of key processes in the cell, such as signalling or gene regulation (1–10). The inherent stochasticity of these biochemical processes is due to the low number of molecules involved in the reactions, leading to intrinsic fluctuations and the breakdown of models based on the Law of Mass Action (11). A number of stochastic models of gene regulation (12–20) and signalling (21, 22) have been formulated and analyzed numerically with the aim of identifying the sources of randomness, and how noise is controlled and harnessed in the cellular environment.

The starting point for such stochastic descriptions is the Chemical Master Equation (CME), a conservation equation that gives the time evolution of the probability distribution of the state of the system (11):

$$\dot{P}_j(t) = \sum_i W_{ji}P_i(t) - W_{ij}P_j(t). \quad (1)$$

Here $P_j(t)$ is the probability of finding the system in state j at time t and W_{ji} is the transition rate from state i to state j . Although theoretically rigorous, there are very few systems for which the CME has been solved analytically. Furthermore, the stiffness of the CME makes direct numerical integration difficult and approximative numerical schemes must normally be employed. In certain limits, one can consider continuum approximations leading to partial differential equations, such as van Kampen's Linear Noise Approximation and Fokker-Planck equations (11). However, these approximations disregard the discreteness of the state of the system, and can therefore give rise to significant deviations when the number of molecules is very small, as can be the case for GRNs.

Gillespie's Stochastic Simulation Algorithm (SSA) (23), by far the most popular numerical method to deal with the CME, follows a different approach. The SSA is a kinetic Monte Carlo algorithm, rigorously derived from the same assumptions as the CME, which gives realizations of the trajectory of a given CME. The SSA provides an *exact* procedure for the kinetic sampling of the CME (24) in the sense that we obtain an unbiased and convergent estimate of the solution of the CME. Due to its biological applications, there has been considerable interest in the SSA in recent years and several extensions have been proposed (e.g., the explicit introduction of spatial variables (25) and time-delays (18)), as well as algorithmic speed-up improvements (26, 27).

In many experiments of interest (5, 6, 9, 10), and in related theoretical analyses (12, 14, 15, 17, 21, 28, 29), the system at hand is assumed to have reached the stationary distribution, i.e., the left hand side of Eq. 1 is zero. Consider the CME (Eq. 1) in operator form:

$$\dot{\mathbf{P}} = W\mathbf{P} - \text{diag}(\mathbf{e}^T W)\mathbf{P} \equiv Q^T \mathbf{P}, \quad (2)$$

where \mathbf{P} is a (possibly infinite-dimensional) column vector of probabilities, \mathbf{e} is the vector of ones, and W is the transition matrix. The stationary distribution \mathbf{P}^*

(usually denoted π in Markov theory) could in principle be obtained from the first left eigenvector of the Q -matrix (30). However, this approach is impractical due to the curse of dimensionality: the run-time and memory requirements scale exponentially with the number of types of molecules. For small state spaces, one can still consider a (truncated) finite subspace to obtain an approximate convergent solution. Our own accurate version of this *approximate eigenvector method* is used in this paper to check the accuracy of our DCFTP-SSA algorithm when an analytical expression for the stationary distribution is not known.

In order to sample the stationary solution of Eq. 1, one would have to run the SSA for an ‘infinite’ time. Of course, the most common practical solution is to run the algorithm ‘repeatedly’ for a ‘very long time’ and hope that the system has reached the stationary distribution when the run is stopped (19). The lack of a termination certificate can lead to computational inefficiency if the runs are longer than necessary or, more importantly, to mis-sampling from the wrong distribution if the runs are not long enough.

In this paper we present an algorithm (DCFTP-SSA) that guarantees *perfect sampling* of the stationary solution of the CME for the general class of biochemical networks formed by the interconnection of generalized Hill- and Monod-type reactions, the canonical models for GRNs and enzymatic networks. The DCFTP-SSA builds on the standard SSA and considers it in the light of Markov Chain Monte Carlo (MCMC) algorithms, specifically within the Dominated Coupling From The Past (DCFTP) framework introduced by Propp and Wilson (31) and Kendall (32). We introduce the algorithm and its properties in detail through the analysis of the building blocks of GRNs. We then apply the DCFTP-SSA to the study of two systems of experimental interest in synthetic biology: the toggle switch (5) and the repressilator (4).

The Dominated Coupling From The Past – Stochastic Simulation Algorithm (DCFTP-SSA)

In many applications we are interested in sampling from a complicated distribution that cannot be written down explicitly. Markov Chain Monte Carlo (MCMC) methods can sometimes provide an answer by setting up a Markov chain which has the desired distribution as its stationary distribution. Sampling from the target distribution is then achieved by evolving the Markov chain until it has reached its stationary distribution (30). The major issue in these schemes is when to stop the Markov chain. This problem was addressed by Propp and Wilson with their Coupling From The Past (CFTP) algorithm (31), a celebrated example of what are commonly referred to as *Perfect Sampling* algorithms (33). The version used here is the Dominated Coupling From The Past (DCFTP) algorithm, the extension introduced by Kendall (32) to study continuous-time Markov chains on an unbounded state space. We now give a brief introduction to the algorithm.

In principle, a Markov chain would have to be run for an infinite time in order to reach its stationary distribution. The CFTP algorithm, however, recasts the problem

as a procedure in which the running time becomes a random variable but a certificate is issued if the stationary distribution has been reached. This is signalled by the coalescence of relevant coupled Markov chains. Markov chains are *coupled* if they use the same sequence of random numbers for their realization and are said to *coalesce* when they meet. Clearly, coupled chains with the same transition rule (but started from different initial states) will have the same values for all future times after the coalescence time T_c . Propp and Wilson proposed to use Markov chains *coupled from the past* to ensure that the whole state space of initial conditions maps to the same state at present. By extending sufficiently far back into the past, we will eventually reach a time from which all paths map to the same state at $t = 0$. This condition is equivalent to the stationary distribution, since the starting condition is irrelevant for the current state. In many systems, the state space is very large, making it infeasible to monitor all paths and their coalescence. However, the situation is much simpler if the state space is partially ordered and we have a *monotone* transition rule ϕ , such that $\phi(x, R) \leq \phi(y, R)$ if $x \preceq y$, where \preceq denotes the partial ordering, x and y are states and R is a random number used to determine the transition. In this case, we only need to monitor two paths: an upper path U and a lower path L , since all other paths lie in between and will coalesce when U and L have done so. This ‘sandwiching’ property is illustrated in Fig. 1. The guaranteed sampling of the CFTP scheme comes with a trade-off: the run time is unbounded, since T_c is itself a random variable which is finite almost surely. If the run is prematurely terminated by an impatient user, the sample will be biased.

Gillespie’s SSA implements a continuous time Markov process with a state space that fulfils the requirements of partial ordering and monotonicity. Therefore, it can be reformulated in the CFTP framework. If the system has a fixed (or bounded) number of molecules, the upper path is trivial and the standard CFTP can be directly applied to the SSA. However, in most situations the state space (i.e., the number of molecules) is unbounded and we must instead employ Kendall’s Dominated CFTP algorithm (32). The DCFTP relies on finding a reversible dominating process D which bounds the original process from above and for which the stationary distribution is known. To create a dominating process, we exploit the reversibility and stationarity of D : start the chain \tilde{D} at $t = 0$ from the stationary distribution and evolve it until $t = T$; then use $D_{-t} = \tilde{D}_t$ as the dominating process on the interval $[-T, 0]$. It then follows that *all* chains of the original dominated process started at $t = -\infty$ will be less than or equal to D at time $-T$ and, consequently, chains coupled to D started from a state $U_{-T} \preceq D_{-T}$ can be interpreted as random realizations of the original (dominated) process started from $t = -\infty$.

Based on the discussion above, a perfect sampling DCFTP-SSA can be developed if two pre-requisites are fulfilled. Firstly, the underlying network of chemical reactions must be reversible, an assumption of broad generality since irreversible reactions are idealizations. Secondly, we must find a dominating process for the particular CME with a known stationary distribution. We will show below that this requirement can be fulfilled for genetic and enzymatic networks formed by the interconnection of Hill-type, Monod-type and linear enzymatic reactions. Our construction is based on the fact that the CME of networks of Hill-type or Monod-type elements can be bounded

from above by processes based on networks of first order reactions, for which the stationary distribution is known to be the multivariate Poisson (34).

A brief outline of the DCFTP-SSA is as follows:

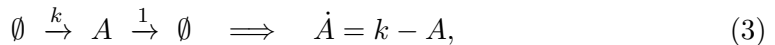
1. Run the dominating process \tilde{D} with known stationary distribution forward in time from $t = 0$ until $t = T$.
2. Apply time-reversal to the stationary process \tilde{D} to obtain the dominating process D such that $D_t = \tilde{D}_{-t}$ from $t = -T$ to $t = 0$.
3. Start upper (U) and lower (L) chains of the original process starting from $U_{-T} = D_{-T}$ and $L_{-T} = 0$ and update each chain *coupled* to D until $t = 0$.
4. If the chains have coalesced at $t = 0$, the common value $U_0^* = L_0^*$ is a sample from the target distribution \mathbf{P}^* .
5. If coalescence has not occurred, double the running time to $t = 2T$ reusing the random numbers from the previous iteration and repeat.
6. Keep doubling the running time until coalescence has occurred at $t = 0$.

The main feature of the DCFTP-SSA is that we are automatically notified that the sampling Markov chain has reached the stationary distribution, and will consequently remain at the stationary distribution for all future times. The DCFTP-SSA can be used to provide a certificate for correct sampling, which can be of importance in high-dimensional systems where the SSA simulations can converge slowly. In addition, we can use the algorithm to discard the ‘burn-in’ period in stochastic simulations by running the DCFTP-SSA until stationary sampling is guaranteed and then continuing with the ordinary SSA from time $t = 0$ onwards. This is important for the numerical study of stationary properties of systems with high variability, e.g., with underlying oscillatory or excitatory behaviour. We present examples of these applications in the sections below.

Detailed application to the first order reaction

In order to illustrate the DCFTP-SSA, we study in detail the simple one-dimensional first order reaction, for which a full *time-dependent analytical* solution of the CME is available. This allows us to study the convergence of the algorithm, as compared to the standard SSA, and to explore the difference between two sources of error which often get entangled: finite sampling error and the mis-sampling error due to the fact that we may not have reached the true stationary distribution.

Consider the simple first order reaction, which has been used as a very simplified description of transcription and translation (2, 17):



where species A is created at a (normalized) constant rate k from a source (\emptyset) and degraded to a sink (\emptyset). The corresponding CME is

$$\dot{P}_j = kP_{j-1} - kP_j + (j+1)P_{j+1} - jP_j \equiv (\mathbb{E}^{-1} - 1)kP_j + (\mathbb{E} - 1)jP_j, \quad (4)$$

with P_j denoting the probability of having j molecules of A . \mathbb{E} and \mathbb{E}^{-1} are the step operators defined by van Kampen (11): $\mathbb{E}f(j) = f(j+1)$ and $\mathbb{E}^{-1}f(j) = f(j-1)$ for a function $f(j)$.

Equation 4 is one of a few CMEs for which the analytical expression of the stationary solution is known (11, 34): it is the Poisson distribution with parameter $\lambda = k$. More importantly for our purposes, one can obtain the full *time-dependent solution* of the CME (see Appendix A). For the usual initial condition with 0 molecules, the time-dependent distribution $\mathbf{P}(t)$ is given by (see Fig. 2 inset):

$$P_j(t) \equiv P(j, t|0, 0) = \frac{\exp(-k(1 - e^{-t}))}{j!} [k(1 - e^{-t})]^j, \quad (5)$$

which converges to the correct stationary distribution as $t \rightarrow \infty$.

The mis-sampling error can be understood analytically in this simple example. If the standard SSA is used to estimate the stationary solution of the CME (Eq. 4), N samples from independent SSA runs will be collected at a stopping time t_{SSA} . This leads to the sampled distribution $\mathbf{P}_{\text{SSA}}(N, t_{\text{SSA}})$, which clearly converges to the stationary distribution \mathbf{P}^* in the double limit $t_{\text{SSA}}, N \rightarrow \infty$. As N is increased, with fixed t_{SSA} , we sample with increasing Monte Carlo accuracy from $\mathbf{P}(t_{\text{SSA}})$ given by Eq. 5 but not from the true stationary distribution \mathbf{P}^* . We therefore reach an error floor that cannot be broken. Using the analytical expression (Eq. 5), the asymptotic error floor $\epsilon_E^*(t_{\text{SSA}})$ is shown to be

$$\begin{aligned} \epsilon_E^*(t_{\text{SSA}})^2 &= \sum_{j=1}^{\infty} (P_j^* - P_j(t_{\text{SSA}}))^2 = \sum_{j=1}^{\infty} \left(\frac{e^{-k} k^j}{j!} - \frac{e^{-\alpha k} (\alpha k)^j}{j!} \right)^2 \\ &= I_0(2k)e^{-2k} - 2I_0(2k\sqrt{\alpha})e^{-k-\alpha} + I_0(2k\alpha)e^{-2\alpha}, \end{aligned} \quad (6)$$

where $\alpha = 1 - e^{-t_{\text{SSA}}}$ and $I_0(x)$ is the modified Bessel function of the first kind. Fig. 2 shows that the levelling-off of the Euclidean error for $\mathbf{P}_{\text{SSA}}(N, t_{\text{SSA}})$ is explained by the error floors calculated from Eq. 6.

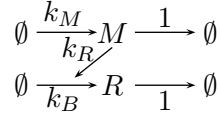
This source of error is eliminated in a DCFTP-SSA formulation of this process. The key step is to find a reversible dominating process with known stationary distribution. In this example, it is clear that the best choice is to use the process (Eq. 4) itself, i.e., the U and D chains in Fig. 1 will be identical. Figure 2 shows the Euclidean error for the DCFTP-SSA sample distribution, which shows no flooring and the expected $N^{-1/2}$ scaling with the number of Monte Carlo runs (35). Equivalent results are obtained with other error measures for the sampled distribution, e.g., the Kullback-Leibler and Kolmogorov distances, and the χ^2 -goodness of fit.

The building blocks: networks and nonlinear elements

In order to extend our study to GRNs, we need to consider how to deal with two key ingredients: networks of reactions, and nonlinear elements of the Hill and Monod types.

Application to networks: Simple gene model of two coupled first order reactions

To showcase how to apply the DCFTP-SSA to networks of several species, we use a widely studied, simplified model of gene expression (13, 16, 17). In its simplest form, the model consists of two types of molecules: mRNA (M) and proteins (R), which are produced and depleted at constant rates. In addition, the mRNA catalyzes protein production through a linear enzymatic reaction:



The deterministic description is given by

$$\begin{aligned} \dot{M} &= k_M - M \\ \dot{R} &= k_B + k_R M - R, \end{aligned} \tag{7}$$

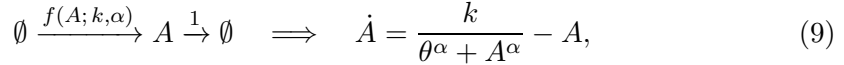
and the corresponding CME is

$$\begin{aligned} \dot{P}_{M,R} &= (\mathbb{E}_M^{-1} - 1)k_M P_{M,R} + (\mathbb{E}_M - 1)M P_{M,R} \\ &+ (\mathbb{E}_R^{-1} - 1)(k_B + k_R M)P_{M,R} + (\mathbb{E}_R - 1)R P_{M,R}. \end{aligned} \tag{8}$$

In fact, Eq. 8 has been solved: the stationary state of the CME of any general network of linear reactions is a multivariate Poisson distribution (16, 34). This means that, similarly to the one-dimensional first order reaction, the DCFTP-SSA is directly applicable to Eq. 8, since the reaction network is reversible and the multivariate Poisson stationary solution is itself a dominating process for the system. The existence of an analytical solution allows us to check how the accuracy of the DCFTP-SSA depends on the dimensionality of the system. Fig. 3 (inset) shows that the marginal distribution (for M) converges like the one dimensional reaction in Fig. 2, with similar error floors for the standard SSA. Note, however, that the joint distribution (Fig. 3) exhibits slower convergence of the standard SSA due to the higher dimensionality of the system, indicating the need for longer SSA runs to avoid mis-sampling from the true distribution. The DCFTP-SSA shows $N^{-1/2}$ Monte Carlo scaling with no error floors regardless of the dimensionality of the system.

Non-linear elements: Hill and Monod reactions

The *Hill reaction* is widely used to model the sigmoidal (non-linear) characteristics of many biological processes and specifically those involved in genetic regulation (4, 5, 36). This model incorporates negative feedback, whereby the rate of creation of new molecules decreases as their concentration increases:

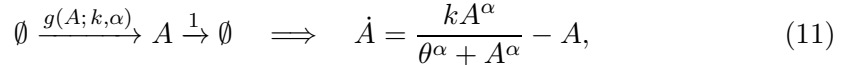


where $f(A; k, \alpha) = k/(\theta^\alpha + A^\alpha)$ is the state-dependent reaction rate, k is the renormalized reaction constant and α is the cooperativity factor (37). Eq. 9 can be derived from elementary Law of Mass Action kinetics through elimination of variables (14). The corresponding CME is given by:

$$\dot{P}_j = (\mathbb{E}^{-1} - 1) \frac{k}{\theta^\alpha + j^\alpha} P_j + (\mathbb{E} - 1) j P_j. \quad (10)$$

It is usual to fix $\theta = 1$ and we do so in the following. For the particular case $\alpha = 1$, Eq. 9 reduces to the familiar Michaelis-Menten equation, for which we can obtain the following analytical expression for the stationary distribution (see Appendix B): $P_j^* = ck^j/(j!)^2$, where $c = 1/I_0(2\sqrt{k})$ is a normalization constant.

The *Monod reaction* is used to model gene upregulation, as referred in particular to the auto-catalysis common in many eucaryotes (10, 36). The reaction can be written as



where $g(A; k, \alpha) = kA^\alpha/(\theta^\alpha + A^\alpha)$ is the state-dependent reaction rate that encapsulates the positive feedback. The corresponding CME is given by

$$\dot{P}_j = (\mathbb{E}^{-1} - 1) \frac{k j^\alpha}{\theta^\alpha + j^\alpha} P_j + (\mathbb{E} - 1) j P_j. \quad (12)$$

Again, we fix $\theta = 1$ in the following. The stationary distribution of the Monod CME (Eq. 12) with $\alpha = 1$ can be obtained analytically (see Appendix B): $P_j^* = ck^j/j!$, with normalization constant $c = 1/(e^k + k - 1)$.

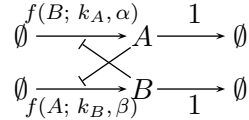
For general α , no explicit solution for the stationary distribution of the CMEs Eq. 10 and Eq. 12 is known, and numerical methods are therefore necessary. Fortunately, the DCFTP-SSA is directly applicable to the reversible Hill and Monod CMEs: the first order reaction, studied in detail in the previous Section, can be used to produce a dominating process for both processes. To see this, note that Eq. 10 and Eq. 12 have birth rates that are bounded from above by k at all times. It is thus straightforward to make sure that the upper and lower paths have rates that fulfill the requirements of the algorithm. As an illustration, Fig. 1 shows one DCFTP-SSA run for the Hill CME (Eq. 10), where D corresponds to the dominating first order linear process (Eq. 4) and U and L are the coupled Hill processes (32, 33). Our detailed simulations of the Hill and Monod CMEs (data not shown) show $N^{-1/2}$ convergence of the DCFTP-SSA unaffected by the mis-sampling errors that can appear when using the standard SSA with short stopping times.

Application to nonlinear models of Gene Regulatory Networks

Our foregoing discussion clarifies why the DCFTP-SSA is applicable to reversible GRNs consisting of interconnected linear enzymatic, Hill and Monod reactions: it is possible to define a dominating process for these networks based on the associated linear network for which the stationary solution (a multivariate Poisson distribution) is known. We now apply our scheme to two recent, canonical examples of synthetic GRNs: a bistable genetic toggle switch (5), with a bimodal stationary distribution; and the repressilator (4), a simple synthetic oscillator.

Toggle switch: two coupled Hill equations

An important characteristic of biochemical networks is the possibility of multistability (1, 5, 12, 14, 17, 19, 38), as exemplified by the toggle switch designed by Gardner *et al* by combining two mutually repressing genes (5, 12, 14, 15, 19). This leads to a bistable system with a sharp switching threshold:



A deterministic model can be derived using two coupled Hill-equations:

$$\begin{aligned} \dot{A} &= \frac{k_A}{1 + B^\alpha} - A \\ \dot{B} &= \frac{k_B}{1 + A^\beta} - B, \end{aligned} \quad (13)$$

where A and B are the molecular numbers of the transcription factors. With appropriate cooperativity factors $\alpha, \beta > 1$ and reaction constants k_A and k_B , Eq. 13 has two stable fixed points (5).

The corresponding CME is given by

$$\begin{aligned} \dot{P}_{A,B} &= (\mathbb{E}_A^{-1} - 1) \frac{k_A}{1 + B^\alpha} P_{A,B} + (\mathbb{E}_A - 1) A P_{A,B} \\ &+ (\mathbb{E}_B^{-1} - 1) \frac{k_B}{1 + A^\beta} P_{A,B} + (\mathbb{E}_B - 1) B P_{A,B}. \end{aligned} \quad (14)$$

Based on our discussion above, it is easy to see that linear process with constant birth rates k_A and k_B will be a dominating process for Eq. 14. However, we need to choose carefully the upper path for the DCFTP-SSA. The key issue is that starting the upper path U from D_T will not give the correct result. This can be understood by considering two paths U and N with A_U and $A_N < A_U$ number of A molecules, respectively. When creating a B molecule, the respective propensities are

$W_U = k_B/(1 + A_U^\beta)$ and $W_N = k_B/(1 + A_N^\beta)$ which implies $W_U < W_N$. This would violate our assumptions about monotonicity. This is easily addressed by considering two upper paths $U_A = (D_{-T,A}, 0)$ and $U_B = (0, D_{-T,B})$. It then follows that any path N will be bounded from above by $U = \max(U_A, U_B)$. Because of their coupling, $U = U_A = U_B$ after the paths have coalesced at time T_U . Consequently, any path N coupled to U_A or U_B will be bounded by U after T_U . As before, complete coalescence occurs when $U = L$.

We have applied the DCFTP-SSA to Eq. 14 to obtain the stationary distribution of the system, which is clearly bimodal (Fig. 4). Because there is no analytical solution in this case, we have checked the accuracy and convergence of the DCFTP-SSA against the approximate eigenvector method with excellent results (not shown).

Beyond certifying proper convergence, the DCFTP-SSA can be used to study properties of the network that need to be properly averaged over the stationary distribution. Consider the mean time for the system to switch from the basin of one fixed point $A^\#$ to the other $B^\#$, i.e., the escape time of the CME (Eq. 14). If the standard SSA were to be used, it would be unclear how to collect proper Monte Carlo statistics, since no certificate of stationarity exists. In contrast, we use a mixed scheme in which an initial DCFTP-SSA run is followed by a (faster) SSA run. The initial DCFTP-SSA run ensures that the *initial condition* for the SSA run is correctly sampled from the stationary distribution at $t = 0$, in essence eliminating the ‘burn-in’ period. From that point onwards, a standard SSA run is performed to obtain statistics of the average time to cross the separatrix. The results are reported in Fig. 4.

In their experiments, Gardner et al. (5) were able to induce faster $A^\# \rightarrow B^\#$ switching by reducing the downregulation capability of A in the cellular environment. This can be mimicked by a modified CME in which the A^β -term in Eq. 14 is removed. If we run the SSA of this modified CME starting from the stationary distribution of the original system (Eq. 14), the escape time $\tau_{A^\# \rightarrow B^\#}$ becomes approximately two orders of magnitude smaller, in broad agreement with the experiment. In fact, it can be shown that the stationary distribution of the modified CME becomes unimodal, with no observable peak for species A .

Repressilator: six-dimensional system of linear enzymatic and Hill equations

The repressilator, a synthetic system of transcriptional regulators, is perhaps the simplest biochemical oscillator that has been implemented experimentally (4). It consists of three genes in a loop, in which the expression of one gene is inhibited by the product of another gene in succession (Fig. 5a):

$$\begin{aligned} \dot{M}_i &= \frac{k_M}{1 + R_{i+1}^\alpha} - d_M M_i \\ \dot{R}_i &= k_B + k_R M_i - R_i, \quad i = 0, 1, 2 \pmod{3}. \end{aligned} \quad (15)$$

Here M_i are the mRNA levels (with production rate k_M and degradation rate d_M) and R_i are the corresponding proteins (with basal rate k_B and linear production

rate k_R). This model of the repressilator is therefore a network of linear enzymatic elements (Eq. 8) for the protein production terms and Hill reactions (Eq. 10) to modulate the production of mRNA. The deterministic system (Eq. 15) has been shown to be oscillatory, with the concentrations of the three proteins peaking in succession (Fig. 5b, top panel).

The corresponding CME is given by

$$\begin{aligned}\dot{P}_n = & \sum_{i=0}^2 (\mathbb{E}_{M_i}^{-1} - 1) \frac{k_M}{(1 + R_{i+1}^\alpha)} P_n + (\mathbb{E}_{M_i} - 1) d_M M_i P_n \\ & + (\mathbb{E}_{R_i}^{-1} - 1) (k_B + k_R M_i) P_n + (\mathbb{E}_{R_i} - 1) R_i P_n,\end{aligned}\quad (16)$$

where the shorthand P_n denotes the state $P_{M_0, M_1, M_2, R_0, R_1, R_2}$ and $i \bmod 3$. We have simulated this six dimensional system with the mixed scheme explained above: we use the DCFTP-SSA to discard the ‘burn-in period’, i.e., the time it takes for the Markov process to reach the stationary distribution, such that the initial conditions for the SSA runs are sampled from the stationary distribution. As a measure of the stationarity of our DCFTP-SSA initialized sampling, we have checked its ergodicity by establishing through an F-test that the average period and amplitude of several short simulations are statistically indistinguishable from those obtained from one long simulation.

As can be seen in the sample trajectory in Fig. 5b, the stochastic system is extremely noisy but it retains the overall oscillation of the genes in succession. The oscillations do not die out even for very long simulations and we have collected statistics of such long runs. Fig. 5c shows a robust feature of the oscillator: the distribution of the period is well fitted by a generalized Gamma distribution, which is characteristic of excitatory systems with a refractory period. The oscillatory behaviour is present for a wide range of the parameters k_M, k_R, d_M (39), which could be modified experimentally. Fig. 5d summarizes our investigation of the robustness of the repressilator to parametric variation. Note the good agreement of the calculated mean period with the corresponding deterministic values. The simulations show that changes in parameters k_M and k_R produce a similar, small effect on the period. The system is, however, more sensitive to parametric changes in d_M . The evaluation of how these parametric variations could be used for the design of tunable and reliable oscillators will be the object of further study.

Discussion

In recent years, the importance of stochastic effects in gene regulation has been elegantly demonstrated through experiments. From a theoretical perspective, such systems are usually analyzed numerically with the standard SSA. When studying stationary properties, this raises questions about the sampling of the stochastic process since the standard SSA does not provide explicit guarantees for convergence. The DCFTP-SSA introduced here can be viewed as a reformulation and extension of the Gillespie algorithm that provides a certificate of convergence. This guarantees that

the sampling is indeed from the correct stationary distribution, thereby removing a source of uncontrolled uncertainty from the simulations.

The guaranteed sampling provided by the DCFTP-SSA comes at an extra computational cost. Although for a general system the coalescence time will depend on the topology of the network and the form of the reactions, the CPU overhead is in no way prohibitive and the DCFTP-SSA can be run on an ordinary desktop computer for the systems presented in this paper. An important theoretical feature of the DCFTP-SSA is the fact that its runtime is not bounded. As our simulations show, this issue does not seem to impose practical restrictions on the algorithm. If necessary, however, this issue can be resolved by using FMMR (40), another perfect sampling algorithm, which dispenses with variable stopping times by running the Markov chains for a fixed time and using rejection sampling to discard those simulations that have not reached the stationary distribution.

In its current form, the DCFTP-SSA can be applied to reversible systems for which there exists a dominating process with known stationary distribution. These include not only networks of linear enzymatic, Hill and Monod reactions, but also reactions whose rate equation is a rational function that can be dominated by a linear process. An example of such rational functions is the model for the λ -phage lysis-lysogeny switch (12, 15), which we have also simulated with the DCFTP-SSA (results not shown). In addition, networks of Michaelis-Menten reactions (or rational enzymatic systems (36)) can also be simulated with the DCFTP-SSA. Bimolecular reactions, on the other hand, are not included in this group. However, an approximate solution to deal with this limitation is already at hand: bimolecular reactions can be simulated with a CFTP-SSA by establishing a fixed upper bound to the number of molecules in the system. If the upper bound is large, the error will be small almost surely. Using the CFTP-SSA has additional advantages, as it is computationally simpler and does not require the reaction network to be reversible. Extending the DCFTP-SSA to deal with second order reactions exactly will be a focus of future work.

Acknowledgments: We would like to thank Michael Elowitz for helpful comments about the repressilator, and Matias Rantalainen, Vincent Rouilly and Sophia Yaliraki for valuable discussions and feedback. Research funded by the EPSRC.

A Time-dependent solution of the Master Equation for the one-dimensional first-order reaction

The CME for the one-dimensional first order reaction (Eq. 4) has the same form as a homogenous birth-death process on the non-negative integers. It is also identical to the equation one obtains when studying the length of a $M/M/\infty$ -queue with Poisson arrival and exponential service time (30). Associated with Eq. 4, there exists a family of orthogonal polynomials $\{\varphi_j(x)\}_{j=0}^{\infty}$ with the three term recurrence relation (41):

$$-x\varphi_j(x) = j\varphi_{j-1}(x) - (k+j)\varphi_j(x) + k\varphi_{j+1}(x), \quad (17)$$

where $\varphi_0(x) = 1$ and $\varphi_j(x) = 0$ for $j < 0$. Karlin and McGregor showed that the recurrence relation (Eq. 17) leads to a spectral representation for $P_{ji}(t)$, the transition probability of going from state i to state j in time t :

$$P_{ji}(t) = P_j^* \int_0^\infty e^{-xt} \varphi_i(x) \varphi_j(x) d\phi(x), \quad (18)$$

where $\phi(x)$ is a positive measure on x and P_j^* is the stationary distribution.

The recurrence relation (Eq. 17) is satisfied by the Charlier polynomials with $\phi(x)$ equal to the Poisson distribution (41), i.e., the Charlier polynomials are a family of polynomials which are orthogonal with respect to the Poisson measure on a discrete lattice on the non-negative integers (42). The Charlier polynomial of order i , parameter a and argument x is denoted $C_i(x; a)$.

Using the following bilinear generating form of the Charlier polynomials (43)

$$\sum_{i=0}^{\infty} \frac{z^k}{k!} C_i(m; x) C_i(n; y) = e^z \left(1 - \frac{z}{x}\right)^m \left(1 - \frac{z}{y}\right)^n C_m\left(n; -\frac{(x-z)(y-z)}{z}\right), \quad (19)$$

Lee (44) showed that Eq. 18 can be simplified to give:

$$P_{ji}(t) = \frac{\exp(-k(1-e^{-t}))}{j!} [k(1-e^{-t})]^j (1-e^{-t})^i C_i\left(j; -\frac{k(1-e^{-t})^2}{e^{-t}}\right). \quad (20)$$

The important special case with initial condition given by a δ -distribution at the origin can be simplified even further. If $P_j(0) = \delta(0)$, then $C_0(j; a) = 1$ and Eq. 20 becomes

$$P(j, t|0, 0) = \frac{\exp(-k(1-e^{-t}))}{j!} [k(1-e^{-t})]^j \equiv P_j(t), \quad (21)$$

which is a Poisson distribution with time-varying parameter $k(t) = k(1-e^{-t})$. Therefore, the stationary Poisson distribution $P_j^* = k^j e^{-k} / j!$ is approached exponentially fast.

Note that

$$\lim_{t \rightarrow \infty} P_{ji}(t) = \frac{e^{-k} k^j}{j!}, \quad (22)$$

which is another way of showing that the stationary distribution the process is Poisson no matter what the initial condition is.

B Stationary solution of the Hill and Monod CMEs with $\alpha = 1$

The stationary solution for the Hill CME (Eq. 10) with cooperativity factor $\alpha = 1$, which is equivalent to the Michaelis-Menten reaction, can be obtained analytically. This reaction can be viewed as a non-linear birth-death process, which allows us to write the stationary distribution P_j^* as (30)

$$P_j^* = c \frac{\lambda_0 \lambda_1 \cdots \lambda_{j-1}}{\mu_1 \mu_2 \cdots \mu_j}, \quad (23)$$

where λ_i and μ_i are the birth and death rates of state i and c is a normalization constant. Inserting the values from the CME (Eq. 10) we obtain

$$P_j^* = c^{-1} \frac{\frac{k}{\theta} \frac{k}{\theta+1} \cdots \frac{k}{\theta+j-1}}{j!} = c^{-1} \frac{k^j \Gamma(\theta+1)}{j! \Gamma(j+\theta)}, \quad (24)$$

with normalization constant

$$c = \frac{\theta I_\theta(2\sqrt{k}) + \sqrt{k} I_{1+\theta}(2\sqrt{k})}{k^{\theta/2}},$$

where $I_\theta(x)$ are Bessel functions. For the special case of $\theta = 1$, we use a recurrence relation for Bessel functions to simplify the above result to $c_0^{-1} = I_0(\sqrt{2}k)$.

Consider now the Monod CME (12) with $\alpha = 1$:

$$\dot{P}_j = \begin{cases} (\mathbb{E}^{-1} - 1) \frac{kj}{\theta+j} P_j + (\mathbb{E} - 1) j P_j & \text{if } j > 1 \\ k & \text{if } j = 0. \end{cases}$$

Note that the birth rate of the state $j = 0$ is modified to avoid it becoming absorbing. Using the same strategy as for the Michaelis-Menten CME above, one can find the stationary distribution

$$P_j^* = c \frac{\frac{k}{\theta+1} \cdots \frac{k(j-1)}{\theta+j-1}}{j!} = c \frac{k^j \Gamma(\theta+1)}{j! \Gamma(j+\theta)}, \quad (25)$$

with normalization constant $c = k (1 + {}_1F_1(2, 1 + \theta, k))$, where ${}_1F_1$ is Gauss' hypergeometric function.

References

1. Acar, M., A. Becskei, and A. van Oudenaarden. 2005. Enhancement of cellular memory by reducing stochastic transitions. *Nature* 435:228–232.
2. Austin, D., M. Allen, J. McCollum, R. Dar, J. Wilgus, G. Sayler, N. Samatova, C. Cox, and M. Simpson. 2006. Gene network shaping of inherent noise spectra. *Nature* 439:608–611.
3. Blake, W. J., M. Kaern, C. R. Cantor, and J. Collins. 2003. Noise in eukaryotic gene expression. *Nature* 422:633–637.
4. Elowitz, M. B., and S. Leibler. 2000. A synthetic oscillatory network of transcriptional regulators. *Nature* 403:335–339.
5. Gardner, T. S., C. R. Cantor, and J. J. Collins. 2000. Construction of a genetic toggle switch in escherichia coli. *Nature* 403:339–343.
6. Pedraza, J. M., and A. van Oudenaarden. 2005. Noise propagation in gene networks. *Science* 307:1965–1969.

7. Volkson, D., J. Marciniak, W. J. Blake, N. Ostroff, L. S. Tsimring, and J. Hasty. 2006. Origins of extrinsic variability in eukaryotic gene expression. *Nature* 439:861–864.
8. Cai, L., N. Friedman, and X. S. Xie. 2006. Stochastic protein expression in individual cells at the single molecule level. *Nature* 440:358–362.
9. Fung, E., W. W. Wong, J. K. Suen, T. Butler, S. gu Lee, and J. C. Liao. 2005. A synthetic gene-metabolic oscillator. *Nature* 435:118–122.
10. Beckskei, A., B. Séraphin, and L. Serrano. 2001. Positive feedback in eukaryotic gene networks: cell differentiation by graded to binary response conversion. *The EMBO Journal* 20:2528–2535.
11. van Kampen, N. G. 1992. Stochastic processes in physics and chemistry. 2nd edition. Elsevier.
12. Hasty, J., J. Pradines, M. Dolnik, and J. J. Collins. 2000. Noise based switches and amplifiers for gene expression. *Proceedings of the National Academy of Sciences* 97:2075– 2080.
13. Kaern, M., T. C. Elston, W. J. Blake, and J. J. Collins. 2005. Stochasticity in gene expression: from theories to phenotypes. *Nature reviews* 6:451–464.
14. Kepler, T. B., and T. C. Elston. 2001. Stochasticity in transcriptional regulation: Origins, consequences and mathematical representations. *Biophysical Journal* 81:3116–3136.
15. McAdams, H. H., and A. Arkin. 1997. Stochastic mechanisms in gene expression. *Proceedings of the National Academy of Sciences* 94:814–819.
16. Paulsson, J. 2004. Summing up the noise in gene networks. *Nature* 427:415–419.
17. Thattai, M., and A. van Oudenaarden. 2001. Intrinsic noise in gene regulatory networks. *Proceedings of the National Academy of Sciences* 98:8614–8619.
18. Bratsun, D., D. Volkson, L. S. Tsimring, and J. Hasty. 2005. Delay-induced stochastic oscillations in gene regulation. *Proceedings of the National Academy of Sciences* 102:14593–14598.
19. Erban, R., I. G. Kevrekidis, D. Adalsteinsson, and T. C. Elston. 2006. Gene regulatory networks: A coarse-grained, equation-free approach to multiscale computation. *Journal of Chemical Physics* 124. 084106.
20. Swain, P. S., and M. B. Elowitz. 2002. Intrinsic and extrinsic contributions to stochasticity in gene expression. *Proceedings of the National Academy of Sciences* 99:12795–12800.
21. Lai, K., M. J. Robertson, and D. Schaffer. 2004. The sonic hedgehog signalling system as a bistable genetic switch. *Biophysical Journal* 86:2748–2757.

22. Samoilov, M., S. Plyasunov, and A. P. Arkin. 2005. Stochastic amplification and signaling in enzymatic futile cycles through noise-induced bistability with oscillations. *Proceedings of the National Academy of Sciences* 102:2310–2315.
23. Gillespie, D. T. 1976. A general method for numerically simulating the stochastic time evolution of coupled chemical reactions. *Journal of Computational Physics* 22:403–434.
24. Gillespie, D. T. 1992. A rigorous derivation of the chemical master equation. *Physica A* 188:404–425.
25. Stundzia, A. B., and C. J. Lumsden. 1996. Stochastic simulation of coupled reaction-diffusion processes. *Journal of Computational Physics* 127:196–207.
26. Gibson, M. A., and J. Bruck. 2000. Efficient exact stochastic simulation of chemical systems with many species and many channels. *Journal of Physical Chemistry A* 104:1876–1899.
27. Cao, Y., D. T. Gillespie, and L. R. Petzold. 2006. Efficient step size selection for the tau-leaping simulation method. *Journal of Chemical Physics* 124. 044109.
28. Tomioka, R., H. Kimura, T. J. Kobayashi, and K. Aihara. 2004. Multivariate analysis of noise in genetic regulatory networks. *Journal of Theoretical Biology* 229:501–521.
29. Kummer, U., B. Krajnc, J. Pahle, A. K. Green, C. J. Dixon, and M. Marhl. 2005. Transition from stochastic to deterministic behavior in calcium oscillations. *Biophysical Journal* 89:1603–1611.
30. Norris, J. R. 1999. Markov chains. Cambridge University Press.
31. Propp, J. G., and D. B. Wilson. 1996. Exact sampling with coupled Markov chains and applications to statistical mechanics. *Random structures and algorithms* 9:223–252.
32. Kendall, W. S. 1997. Perfect simulation for spatial point processes. In *Bulletin ISI*, 51st session proceedings, volume 3. 163–166.
33. Thöennes, E. 2000. A primer on perfect simulation. In *Springer Lecture Notes in Physics*, K. R. Mecke, and D. Stoyan, editors, volume 554. Springer, 349–378.
34. Gadgil, C., C.-H. Lee, and H. G. Othmer. 2005. A stochastic analysis of first-order reaction networks. *Bulletin of Mathematical Biology* 67:901–946.
35. Shreider, Y. A., editor. 1966. The MonteCarlo Method. Pergamon Press.
36. Cornish-Bowden, A. 2004. Fundamentals of Enzyme Kinetics. 3rd edition. Portland Press.

37. Rosenfeld, N., M. B. Elowitz, and U. Alon. 2002. Negative autoregulation speeds up the response times of transcription networks. *Journal Of Molecular Biology* 323:785–793.
38. Craciun, G., Y. Tang, and M. Feinberg. 2006. Understanding bistability in complex enzyme-driven reaction networks. *Proceedings of the National Academy of Sciences* 103:8697–8702.
39. Scott, M., B. Ingalls, and M. Kaern. 2006. Estimation of intrinsic and extrinsic noise in models of nonlinear genetic networks. *Chaos* :026107.
40. Fill, J. A., M. Machida, D. J. Murdoch, and J. S. Rosenthal. 2000. Extension of fill's perfect rejection sampling algorithm to general chains. *Random Structures and Algorithms* 9:223–252.
41. Karlin, S., and J. McGregor. 1955. Representation of a class of stochastic processes. *Proceedings of the National Academy of Sciences* 41:387–391.
42. Nikiforov, A. F., and V. B. Uvarov. 1991. Classical orthogonal polynomials of a discrete variable. Springer-Verlag.
43. Meixner, J. 1939. Erzeugende funktionen der charlierschen polynome. *Mathematische Zeitschrift* 44:531–535.
44. Lee, P.-A. 1997. Markov processes and a multiple generating function of product of generalized Laguerre polynomials. *Journal of Physics A* 30:373–377.
45. Chung, F. R. K. 1997. Spectral graph theory. American Mathematical Society.

Figure Legends

Figure 1

An illustrative run of the DCFTP-SSA for the Hill equation. The top panel shows the algorithm started from $t = -1$. Both the upper (U) and lower (L) are coupled to the dominating path (D) and here they fail to coalesce before $t = 0$. In the lower panel, the algorithm is restarted from $t = -2$. Note that D extends further into the past but the realization in the interval $t \in [-1, 0]$ is the same as above. In this case, coalescence occurs at $T_c = -0.17$ and the value $U_0^* = L_0^*$ is guaranteed to be a sample from the stationary solution of the Hill CME (Eq. 10).

Figure 2

Comparison of the convergence of the DCFTP-SSA vs. the standard SSA for the first order reaction (Eq. 4) with $k = 5$. We present the Euclidean error of the distribution as a function of the number of Monte Carlo runs N for the DCFTP-SSA (*) and for the standard SSA with stopping times: $t_{\text{SSA}} = 1(\nabla), 2(\diamond), 3(\square), 15(\circ)$. Note that the error of the SSA runs converges to the asymptotic error floors for the different stopping times given by Eq. 6 (dotted lines). The dashed line corresponds to the $N^{-1/2}$ Monte Carlo scaling and shows the correct convergence of the DCFTP-SSA (and the SSA only when the stopping time is with very long). Each point is calculated from the mean of 100 different ensembles of N samples, with numerical error bars smaller than the symbols. *Inset:* The full time-dependent solution of the first order reaction (Eq. 5) from a δ -distribution initial condition. The distribution evolves towards a smoother Poisson distribution. The dark lines correspond to the distributions at $t = 1, 2, 3$ used in the main panel.

Figure 3

The effect of dimensionality on the convergence of the sampled distribution. The main panel shows the Euclidean error for the joint distribution of the linear gene model (Eq. 8) with $k_M = 3$, $k_R = 3$ and $k_B = 1$. The open symbols correspond to the standard SSA with stopping times as in Fig. 2 while the DCFTP-SSA is marked by asterisks. The points are obtained by averaging over 100 ensembles of N samples, with error bars contained within the symbols. The higher dimensionality and the topology of the network make the convergence of the standard SSA much slower for this case than for the one-dimensional first order reaction in Fig. 2. Note that the DCFTP-SSA is unaffected by error floors and shows $N^{-1/2}$ convergence, as given by the dashed line. *Inset:* Same as the main panel for the marginal distribution of the mRNA (M). In this case, the convergence is as for the one-dimensional linear reaction in Fig. 2. The difference between the convergence of the joint and marginal distributions is not surprising: the production of R is downstream from M and it is unlikely to reach the stationary level before M .

Figure 4

Stationary distribution for the toggle switch (Eq. 14) with parameters $k_A = 30, k_B = 10, \alpha = 3, \beta = 1$. The bimodality of the distribution leads to switching behavior. We have checked that the Euclidean error of the DCFTP-SSA sampled distribution decreases at the expected $N^{-1/2}$ rate (data not shown). The state space can be divided in two regions $A^\#$ and $B^\#$ corresponding to the two basins of attraction of the fixed points. The separatrix is found from the sign of the Fiedler eigenvector of the Laplacian (45) of the state space lattice. The probabilities $P_{A^\#}$ and $P_{B^\#}$ of finding the system in each basin computed with the DCFTP-SSA compare very well with those obtained with the approximate eigenvector method (in parenthesis). Similarly, the expected time to reach the separatrix averaged over all the states in each basin (30) calculated with the DCFTP-SSA (averaged over 25 ensembles, each consisting of 1000 samples) compare well with the approximate eigenvector method (in parenthesis).

Figure 5

Analysis of the repressilator with $k_M = 10, d_M = 1, \alpha = 2, k_B = 1, k_R = 3$. (a) Diagrammatic representation of the repressilator network showing the alternating positive and negative feedbacks. (b) *Top*: One SSA realization of the CME (Eq. 16) started from the stationary distribution showing the concentrations of the three proteins. The oscillations are very noisy and far from sinusoidal. The Fourier spectrum shows no distinguishable peaks (data not shown). *Bottom*: The corresponding deterministic solution (Eq. 15) exhibits regular oscillations of the proteins in succession. (c) Distribution of the period τ at stationarity obtained from a long SSA run. The solid line corresponds to a best fit to a generalized Gamma distribution while the dotted line shows a Poisson distribution with the same mean. (d) Change of the period of the repressilator as a function of parameter variation. There is good agreement between the sensitivity of the stochastic system with respect to a $\pm 5\%$ change in k_M (*), k_P (\square), and d_M (\bigcirc), and the deterministic system (solid lines). The effect of d_M on the duration of the period τ is greater and opposite to that of k_M and k_P , which are similar.

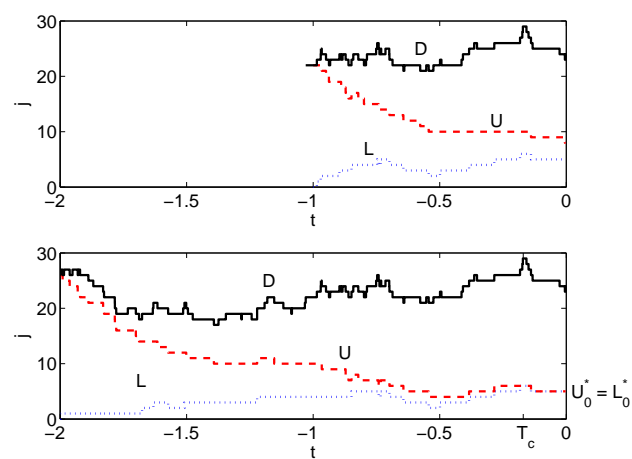


Figure 1:

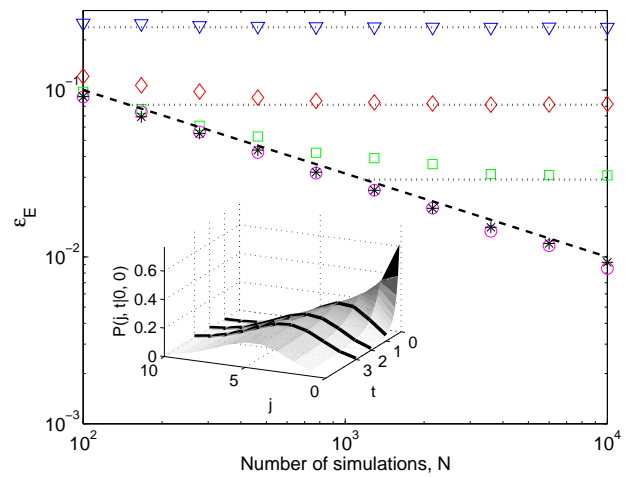


Figure 2:

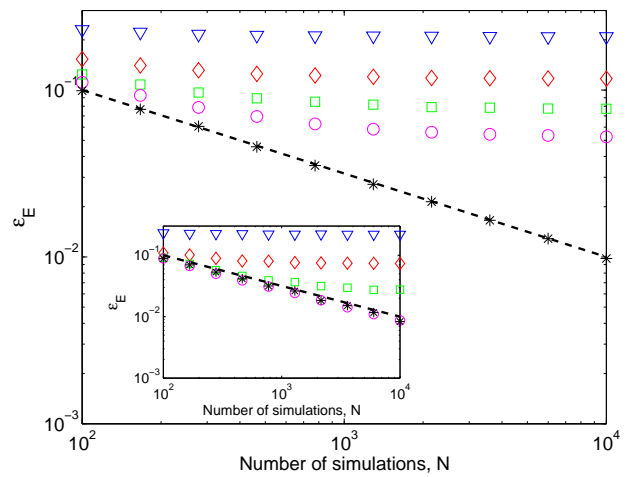


Figure 3:

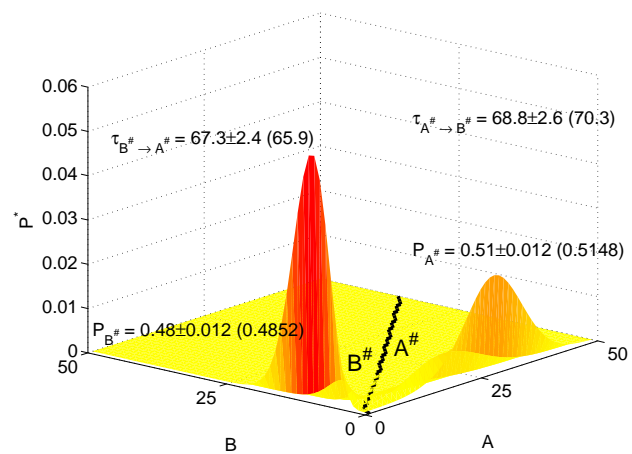


Figure 4:

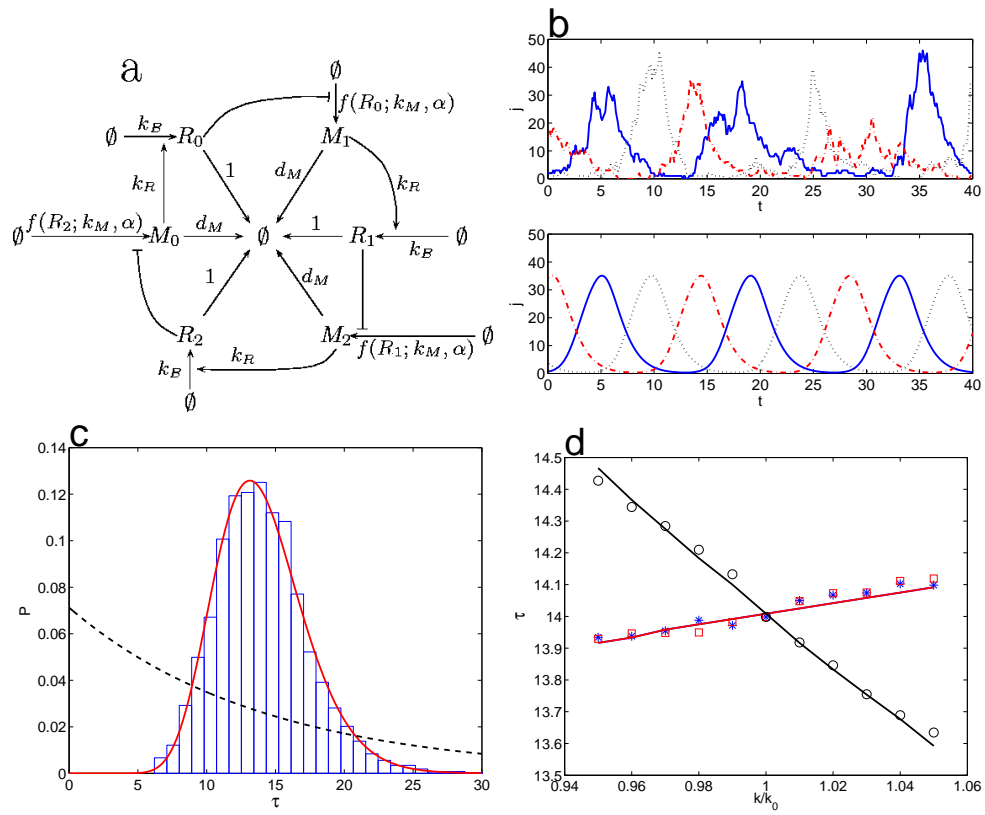


Figure 5: